Scalable solar thermoelectrics and photovoltaics (SUNTRAP)

Tracy K. N. Sweet, Matthew Rolley, Gao Min, Andy Knox, Duncan Gregory, Douglas Paul, Manosh Paul, Andrea Montecucco, Jonathan Siviter, Paul Mullen, Ali Ashraf, Wenguan Li, Tapas Mallick, Nazmi Sellami, Hasan Baig, Xian-long Meng, Robert Freer, Feridoon Azough, and Eduardo F. Fernández

Citation: AIP Conference Proceedings **1766**, 080007 (2016); doi: 10.1063/1.4962105
View online: http://dx.doi.org/10.1063/1.4962105
View Table of Contents: http://scitation.aip.org/content/aip/proceeding/aipcp/1766?ver=pdfcov
Published by the AIP Publishing

Scalable Solar Thermoelectrics and Photovoltaics (SUNTRAP)

Tracy K.N. Sweet[1, a)], Matthew Rolley[1] and Gao Min[1], Andy Knox[2], Duncan Gregory[2], Douglas Paul[2], Manosh Paul[2], Andrea Montecucco[2], Jonathan Siviter[2], Paul Mullen[2], Ali Ashraf[2], Wenguan Li[2], Tapas Mallick[3], Nazmi Sellami[3], Hasan Baig[3], Xian-long Meng[3], Robert Freer[4], Feridoon Azough[4], Eduardo F. Fernández[5]

[1]*Cardiff University, Queen's Buildings, The Parade, Cardiff. CF24 3AA, UK.*
[2]*University of Glasgow, UK.* [3]*Exeter University,UK.* [4]*The University of Manchester, UK.* [5]*University of Jaen, Spain.*

[a)] Corresponding author: Sweett@Cardiff.ac.uk

Abstract. This paper presents the design, manufacture and electrical test of a novel integrated III:V low concentrator photovoltaic and thermoelectric device for enhanced solar energy harvesting efficiency. The PCB-based platform is a highly reliable means of controlling CPV cell operational temperature under a range of irradiance conditions. The design enables reproducible data acquisition from CPV solar cells whilst minimizing transient time for solid state cooling capability.

INTRODUCTION

Concentrator photovoltaics (CPV) use lenses or mirrors to concentrate sunlight to increase the incident photon density onto a small area of a semiconductor photovoltaic (PV) cell, typically 30-100mm^2. There are two main benefits to using CPV, the cost of modules is reduced by exploiting cheap optics which reflect / refract photons onto the receiver assemblies. Additionally, the efficiency of a CPV cell is increased with an increasing optical concentration, until limited by the series resistance of the cell. Previous work has shown that cell temperature has a linear dependence on geometric concentration [1]. Several approaches for cell cooling have been investigated for CPV applications to reduce operational temperature below 80^{o}C [2]. Heat sinks are widely utilised in CPV. These are passive technologies with the advantage of not requiring power input for cooling. They are usually made of aluminium and utilise the metal's high thermal conductivity over a large area to radiate and dissipate waste heat from the CPV cell. However, complex finned heat sink designs can be heavy, expensive and although cell cooling is achieved, cell temperature is not actively controlled. Water-cooled designs are also available, but water circulation close to the cells can be complex, and power input is required to pump water efficiently around the system.

Recently, several papers have been reported in the literature which combine CPV with solid-state thermoelectric (TE) technologies. TE modules have been applied in either Peltier (cooling) or Seebeck (power generation) mode. A model based on bismuth telluride and 14.03% multi-crystalline solar module efficiency was investigated [3]. The contribution of the TE was shown to increase the annual electricity yield of the lone PV module by 11.0-14.7% at 25^{o}C. A low concentration polycrystalline hybrid system with bismuth telluride thermoelectric modules was modelled optimizing load resistance to the system [4]. This work emphasized the importance of both the thermal conductance between the PV cell and the TE module, and the concentration ratio as crucial design factors when designing hybrid systems. It was stated that the performance of the hybrid device, compared with that of the CPV device, was improved significantly. Another integrated device with 300 GaAs/Ge tandem solar cells connected in series, and 300 bismuth telluride couples in a laminated architecture was investigated [5]. It was found that the PV-TE system had a comparable thermal efficiency to an equivalent PV-Thermal system, providing a further 8%

12th International Conference on Concentrator Photovoltaic Systems (CPV-12)
AIP Conf. Proc. 1766, 080007-1–080007-10; doi: 10.1063/1.4962105
Published by AIP Publishing. 978-0-7354-1424-2/$30.00

electrical efficiency relative to the PV technology alone. The electrical efficiency was related to the length of the TE legs, consistent with early work in thermoelectric literature with a focus on module design [6]. An interesting study relating to the geographic location effects on a hybrid PV-TE system were evaluated at multiple European sites [7]. It was found that the high irradiance and low ambient temperature climate in southern European countries would benefit from deployment of an integrated device. Load matching on a hybrid device was investigated and once again shown that the integrated system had the capability of producing more power than the PV cells on their own [8].

Perovskite solar cells have gained increasing attention within the photovoltaic community due to the rapid increase in their generation efficiency. A theoretical study on a hybrid Perovskite-TE device was investigated [9]. It was found that the addition of a TE module added 0.8% to the overall generation efficiency. The use of a thermal concentrator was also an effective way to reduce the system cost, due to an increased hot side temperature and hence requiring a smaller, cheaper TE module. MATLAB was used in a thermodynamic model [10] that simulated a concentrated hybrid system. The design of integrated systems rely on optimal concentration ratio, with integrated CPV-TE devices producing more power output than CPV or TE alone (111W compared with 97.97W and 12.99W respectively). The benefits of changing the internal geometry of the thermoelectric itself within a hybrid system has been modelled [11]. It was shown using MATLAB and COMSOL that the maximum power output of the TE module corresponds to an optimum thermoelement length. Therefore an optimum balance between hybrid system performance, and the design of the included thermoelectric module was deduced. The performance of three hybrid devices was investigated [12]. It was shown that the addition of a selective solar absorber, converting low frequency light into heat, increased the hybrid device's power generation efficiency compared with CPV alone.

A hybrid CPV-TE device utilizing a triple junction solar cell and x200 optical concentration was made and tested [13]. The individual PV and TE were connected to separate circuits to minimize current limiting losses. With increasing concentration in the hybrid system the TE module's relative contribution also increased. The hybrid design produced more power output than the PV alone, at all concentrations. The inherent Thomson effect in the TE lowered the temperature of the hybrid system during operation. The use of a thermal concentrator was further explored with a hybrid design that used a TE with much smaller geometry than that of the PV cell [14]. A mono-crystalline silicon solar cell was combined with four TEs in series which were water cooled, and a 25% performance increase was shown compared to the PV cells alone. A copper block thermal concentrator was used creating a temperature difference of 52^{o}C under illumination of 650Wm^{-2} with a representative cold side temperature of 20^{o}C.

Two types of solar technology were experimentally evaluated in a hybrid device, poly-crystalline silicon and DSSCs. Bismuth telluride thermoelectric modules and a water heat exchanger were used [15]. This work confirmed the results of earlier simulations [11], [5] and suggested that further hybrid designs should attempt to use smaller length thermoelement modules to capitalise on the small temperature differences in CPV-TE devices. The temperature increase of the solar cell was minimized and the hybrid design power generation exceeded that of the sole PV cell in all four cases. The relative improvement to the DSSC hybrid system was 30.2% with the polycrystalline technology showing a 22.5% improvement.

The work in this paper investigates the integration of commercially-available TE Peltier modules with high efficiency III:V triple-junction CPV cells. The design, manufacture and electrical test data for a novel PCB-based integrated III:V CPV-TE solar energy harvesting device is presented.

EXPERIMENTAL

The multi-junction receiver consisted of a novel architecture, a sandwiched 2-PCB structure, allowing robust electrical and thermal testing. The III:V triple junction cell (active area 5.5 mm x 5.5mm) was thermally and electrically contacted to a thermoelectric module, with wirebonded top (n-type) contacts. The integrated PCB-CPV-TE device was mounted on a copper block for accurate temperature measurements. A LOT Oriel LCS-100 94011A solar simulator was used to determine the performance of both the CPV cell and of the TE module. A broadband solar spectrum of AM 1.5G, close to that obtained from the sun, is used with wavelength range from 300 to 2500nm. A Kipp and Zonen CM11 pyranometer was used to measure the global horizontal irradiance, with careful attention given to the angular sensitivity of the instrument. The dome was cleaned to eliminate dirt effects. The perpendicular vertical height between the solar simulator lamp output and the pyranometer was carefully measured. To correctly measure these devices, the 1000W/m^2 standard irradiance plane was measured. The top surface of the CPV cell was then placed at the centre of the irradiance plane to avoid spatial uniformity errors, and to give highly reproducible results. The lamp height was adjusted after the CCPC optics were added to maintain the irradiance plane at the optical entrance to the device. The simulator was switched on 20 minutes before measurements to avoid spectral or

temporal anomalies. The receiver assembly was placed on a water heat exchanger. The temperature of the receiver base was measured using a k-type thermocouple. A thin layer of thermal interface material was applied to maximise thermal conductivity from the device to the heat exchanger. Top solar cell surface temperature measurements were recorded with a FLIR-i7 thermal imaging camera. Contactless thermal and thermocouple measurements allowed evaluation of the thermal characteristics of the CPV-TE receiver without affecting irradiance levels on the cell.

RESULTS AND DISCUSSION

The device integrates a III:V TJ CPV cell and a TE module, with high thermal conductivity designed at each interface (Fig 1). The CPV cell was electrically and thermally bonded to the top surface of the TE module with a very closely-matched device footprint to maximise the thermal interface area whilst maintaining design compactness. The device was manufactured under cleanroom conditions and encapsulated to prevent contamination from atmospheric particles, and hence ensure reliable operation over the device lifetime. A photograph is given in Fig 2.

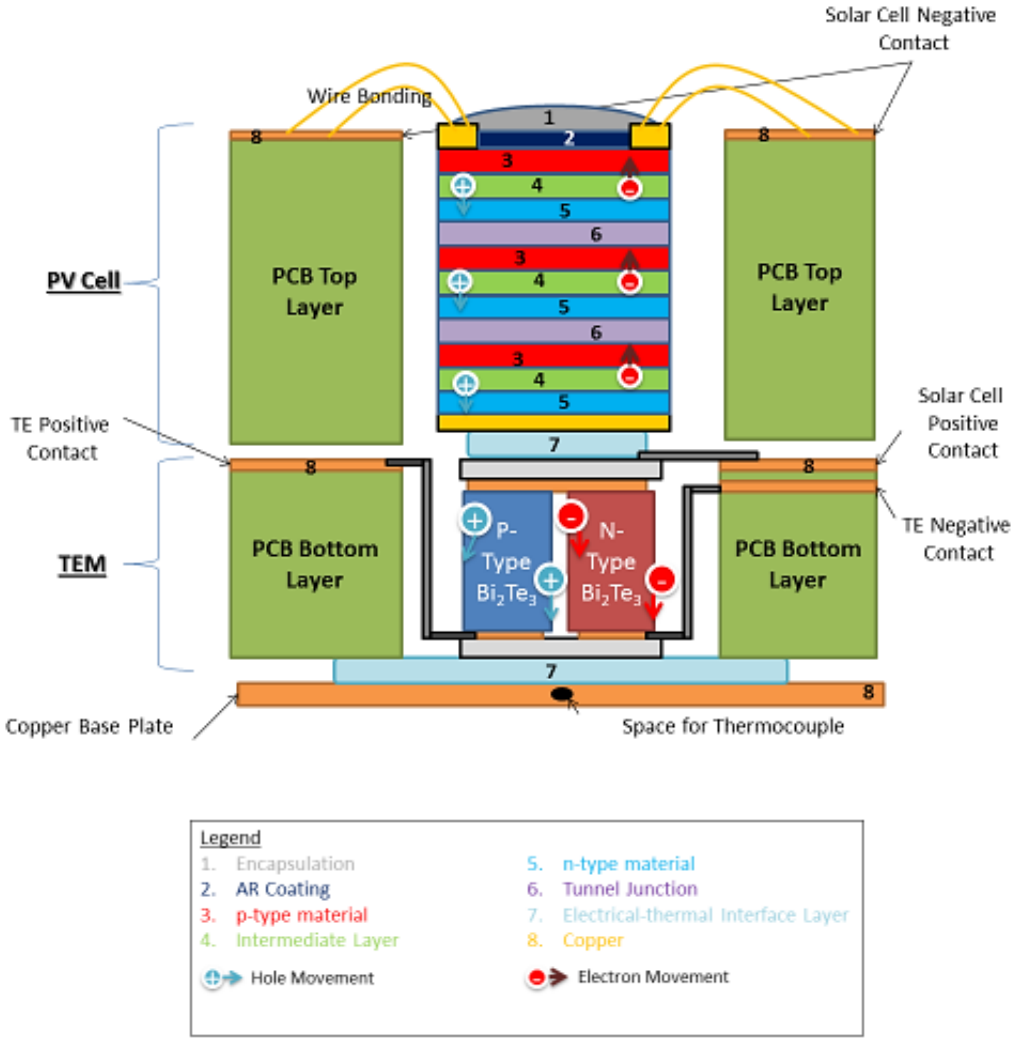

FIGURE 1. An illustrative schematic diagram of the PCB-based CPV-TE receiver device (not drawn to scale)

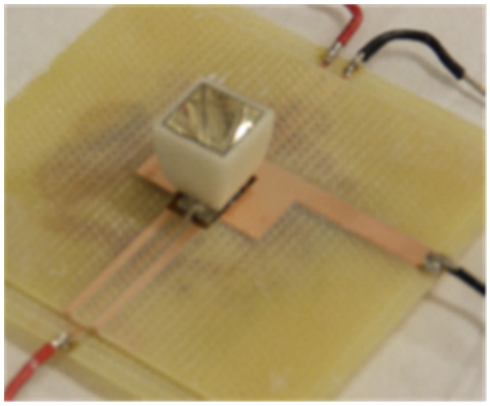

FIGURE 2. A photograph of the manufactured CPV-TE device, with Crossed Compound Parabolic Concentrator optics

Crossed Compound Parabolic Concentrators (CCPC) have been utilised with the PCB CPV-TE device. These inexpensive optics reflect solar photons onto the CPV semiconductor cell surface. Optoelectronic CPV cell efficiency is increased when these concentrating optics are applied. Additional waste heat is generated in the process, see Fig. 3.

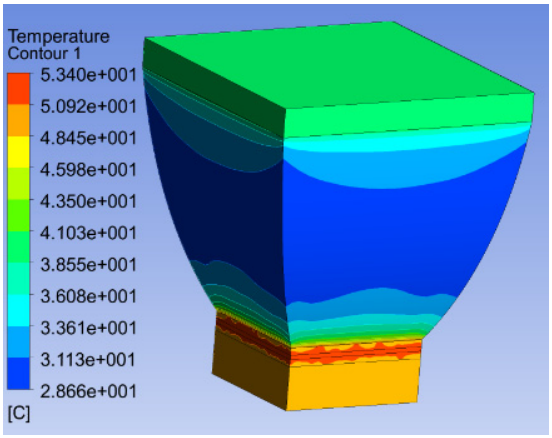

FIGURE 3. ANSYS simulation of CCPC optics showing a maximum temperature of 53^{o}C at the cell surface

The receiver was electrically connected using a four-wire measurement to an AUTOLAB system. I-V characteristics were measured inside of a blackened faraday cage to eliminate any light from the environment. The thermoelectric module was driven using an external power supply, with the current driven to a specific value to obtain the required cell temperature. This control method was used due the proportionality between a thermoelectric module's created temperature difference and supplied current. The integrated receiver was measured with and without the CCPC optics under a 1000W/m^2, AM1.5G spectrum. The measured data are presented as Fig. 4 and Table 1.

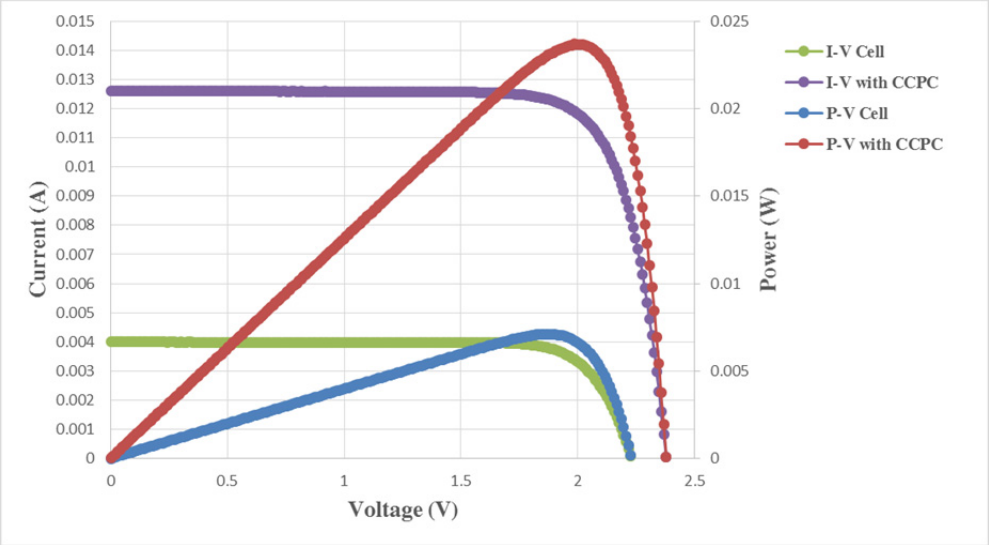

FIGURE 4. Current-Voltage and Power-Voltage data for the CPV-TE receiver with / without CCPC optics

TABLE 1. CPV cell electrical and geometric measurement

Parameter	Bare CPV cell	Cell + CCPC optics
Isc (A)	0.0040	0.0126
Voc (V)	2.2370	2.3780
Fill Factor (%)	79.10	79.40
Maximum power point (W)	0.0071	0.0237
Cell efficiency (%)	23.49	23.83
Optical efficiency (%)		78.8
Active area (mm)	5.5 x 5.5	11 x 11

The optical concentration ratio based on maximum power generation of the CPV cell was calculated as 3.29, slightly less than the theoretical geometrical concentration ratio (Aperture area / Receiver area) of 4.0.
The efficiency of the cell increased by 0.34% after addition of the CCPC optics. The optical efficiency 78.8%, was calculated based on short circuit current (Isc) and theoretical geometrical concentration ratio according to equation (1). The Fill Factor (FF) and Efficiency were calculated according to equations (2) and (3) where Pmpp = power at maximum power point, Voc = open circuit voltage, Isc = short circuit current (A), E = irradiance (W/m^2) and A = active cell area (m^2).

$$\text{Optical efficiency} = [\text{Isc with CPPC}/(\text{Isc bare cell}*CR)]*100 \quad (1)$$

$$FF=[Pmpp/(Voc*Isc)]*100 \quad (2)$$

$$\text{Efficiency}=[Pmpp/(E*A)]*100 \quad (3)$$

The electrical characterisation and specification data for the encapsulated Bismuth Telluride TE module, tested as part of the CPV-TE device, is given in Fig. 5 and Table 2. The internal resistance (Rint) of the TE module (1.23 Ω) was confirmed via in house impedance measurements. It is noted that the thermoelectric capacitance and resistance are defined by temperature, the Seebeck coefficient and the thermal properties of the module [16]. A module with a large number of thermoelectric legs was chosen to drive a high Seebeck voltage in the device. Interestingly, there is a 3.44 increase in power generated from the TE module upon addition of the CCPC optics (86% efficiency calculated based on heat input). The spectral photon energy not converted to electricity combined with thermalisation losses within the CPV cell is efficiently transmitted to the TE module.

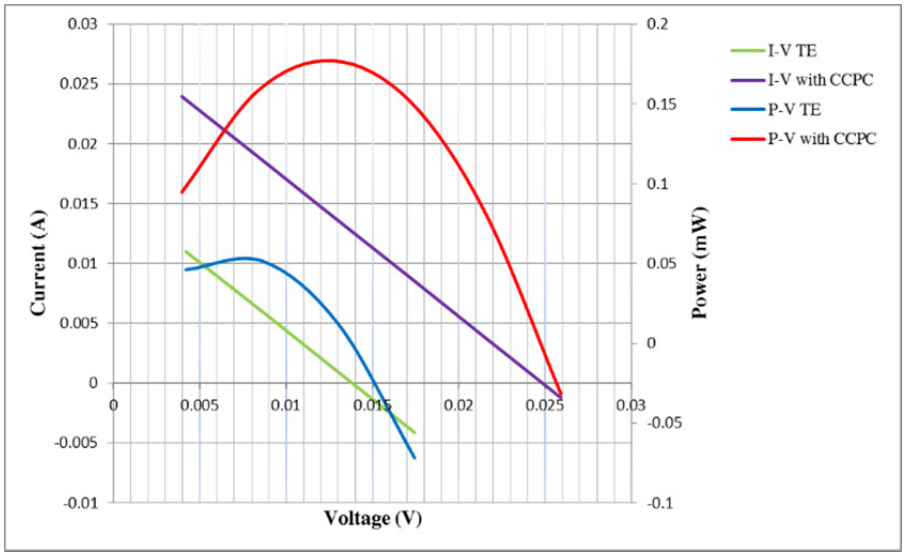

FIGURE 5. TE module Current-Voltage and Power-Voltage data with/without optics

TABLE 2. TE module electrical and geometric measurements.

Parameter	TE module
Number of legs	46
Leg geometry (mm)	0.6 x 0.6
Leg length (mm)	1.20
Module length x width (mm)	8.3 x 6.0
Fill Factor (%)	33.25
Total metallization (mm)	0.3
Rint (Ω)	1.23
MPP (mW) no CCPC	0.0514
MPP(mW) with CCPC	0.1770

Multiple problems were encountered with reliably measuring the temperature of the CPV cell. These issues were due to thermal conductivity of soldered contacts, potential shading of the active area of the CPV cell or interference with the CCPC optics. A contactless thermal imaging camera (FLIR i7) methodology was adopted with a selected emissivity of 0.6. A representative thermal image of the PCB CPV-TE device (Fig. 2) is given in Fig. 6. A minimum of three concurrent images were taken, and the temperature readings averaged to give reliable cell temperature measurements. The TE module was observed to be much more sensitive to CPV cell temperature changes during I-V measurement than a K-type thermocouple. This effect could be utilised for future system development due to rapid response to real-world irradiance/cell temperature changes.

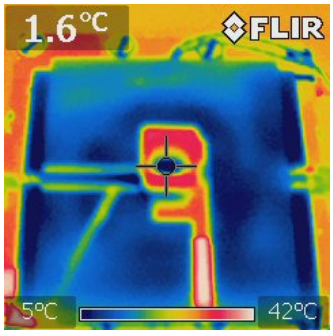

FIGURE 6. FLIR thermal camera image of the CPV-TE receiver – Peltier cooling of the TE module of the CPV cell to 1.6°C

The TE module was successfully and reproducibly used to vary and control the CPV cell's operational temperature from 68°C down to 1.6°C. The Power-Voltage data are given in Fig 7 and Table 3.

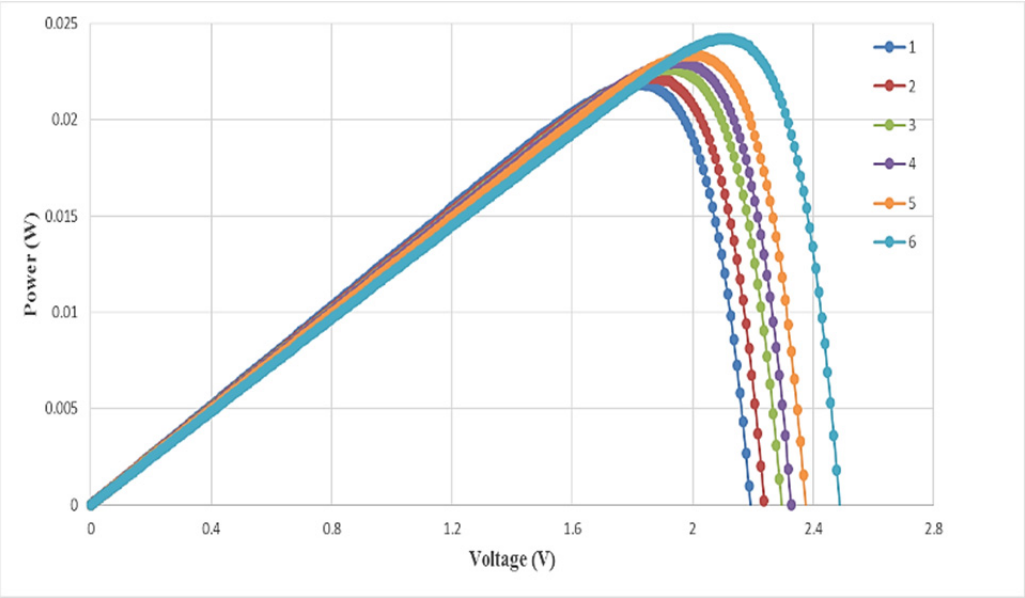

FIGURE 7. Power-voltage curves for the CPV-TE receiver (the cell temperatures are given in Table 3)

TABLE 3. CPV-TE electrical characteristic measurements

Run number	Temp	Isc	Voc	FF	ηeff
	(°C)	(A)	(V)	(%)	(%)
1	68.0	0.01289	2.1864	77.46	21.96
2	52.4	0.01274	2.2368	77.73	22.29
3	41.4	0.01263	2.2871	78.34	22.77
4	33.0	0.01258	2.3274	78.45	23.11
5	9.9	0.01244	2.3777	78.91	23.48
6	1.6	0.01212	2.4886	80.2	24.34

The TE module controlled the CPV cell operating temperature in Peltier mode by current supply. The reduction from 68°C to 1.6°C increased the cell efficiency by 2.38%. The Voc was observed to increase by 13.8% over this temperature range, whilst the Isc decreased by ~6%. The Fill Factor was seen to increase by 2.74% upon cooling by 66.4°C. The temperature coefficient for maximum power output for the III:V triple-junction CPV cell efficiency, under 1000W/m^2 and AM1.5G spectrum, was calculated as -0.162 relative %/K over the temperature range. The temperature coefficient decreases with increasing irradiance, therefore this value is acceptable when compared to literature values of -0.15 to -0.10 relative %/K measured for III:V cells under high concentration (x300 to x500) [17]. The TE module was used to obtain three steady-state CPV cell temperatures at 273K, 298K and 323K under optical concentration. The CPV cell response data with CCPC optics are summarised in Figs. 8 and 9.

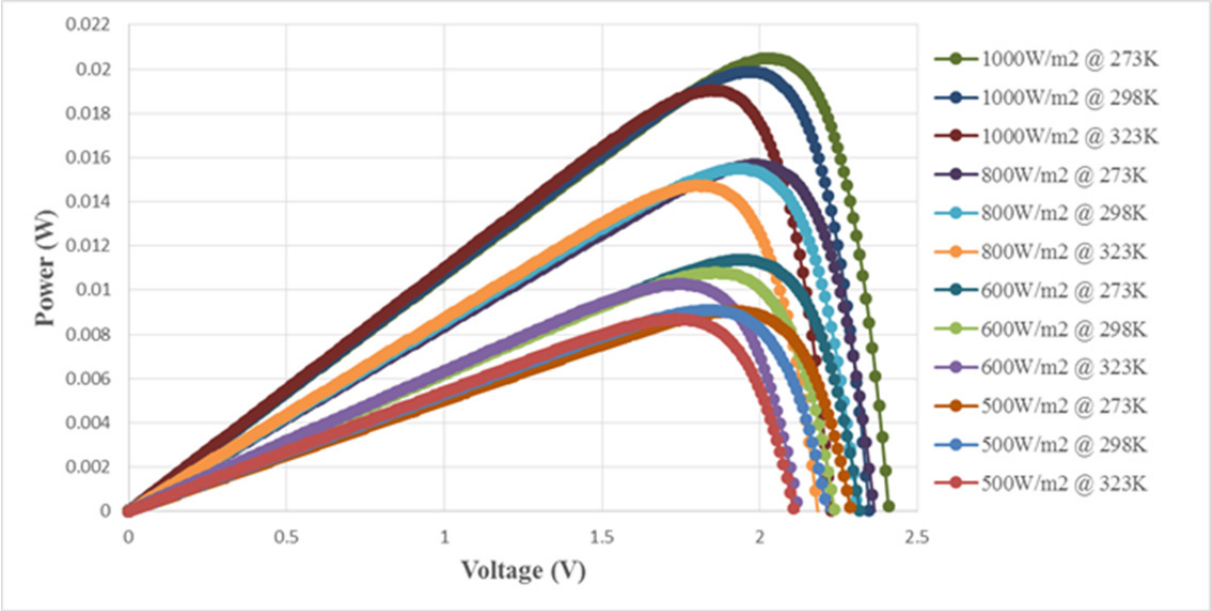

FIGURE 8. Experimental Maximum power output data varying irradiance and temperature.

FIGURE 9. Maximum power point vs irradiance data at 273K, 298K and 323K.

A reproducible trend of increasing Power output with increasing irradiance level (W/m^2), together with temperature reduction, has been shown in Fig 8. The increase in MPP for the four irradiance conditions, upon temperature decrease from 323K to 273K, range from 4.0% to 9.7% (the smallest increase in MPP for the $500W/m^2$ irradiance condition). The plot of MPP vs Irradiance is linear for all three test temperatures, 273K, 298K and 323K. The R-squared values, plotted in Fig. 8(b), are 0.9994, 0.9981 and 0.9978, respectively and show good agreement

with this trend. This data also clearly illustrates the benefit to CPV power generation on cooling the cell from 323K to 273K, particularly at higher irradiance levels, such as under Standard Test Condition, 1000W/m^2.

CONCLUSIONS

A novel integrated CPV-TE PCB-based receiver was designed, manufactured and tested. The mechanically robust PCB design enabled reproducible CPV cell temperature control during electrical characterization. The solid-state Thermoelectric Peltier module reliably reduced the operational III:V CPV cell temperature by 66.4^{o}C, increasing absolute cell efficiency by 2.38%. The temperature coefficient for maximum power output for the III:V triple-junction CPV cell efficiency under STC was calculated as -0.162 relative %/K, in close agreement with literature values. Thermoelectric technology has been shown to conveniently, reproducibly and virtually instantaneously control the operational steady-state CPV cell temperature at different irradiance levels. This work demonstrates the potential of the receiver to reduce operational CPV cell temperature, thereby increasing cell efficiency and lifetime. Future work includes testing under high concentration primary optics (>x500), assessing thermoelectric Seebeck (power generation), scale-up to full modular integrated solar energy harvesting system to optimize solar energy harvesting and energy balance optimization with consideration of climatic factors.

ACKNOWLEDGMENTS

The authors would like to acknowledge the Sêr Cymru National Research Network and EPSRC for financial support. Grateful thanks are extended to Cardiff School of Physics and Astronomy for use of cleanroom facilities and the Electronics workshop for PCB machining.

REFERENCES

1. L.Micheli, E.F..Fernandez, F. Almonacid, T.K. Mallick and G.P. Smestad, Performance, limits and economic perspectives for passive cooling of High Concentrator Photovoltaics. Solar Energy Materials & Solar Cells 153 (2016) 164-178.
2. E.F. Fernandez, F. Almonacid, P.Rodrigo. P. Perez-Higueras, Calculation of the cell temperature of a high concentrator photovoltaic (HCPV) module: a study and comparison of different methods. Sol. Energy Mater. Sol. Cells 121 (2014) 144-151.
3. W. G. J. H. M. Sark, Feasibility of photovoltaic – Thermoelectric hybrid modules. *Applied Energy* 88(8), pp. 2785-2790 (2011). Liao, T. et al. 2014. Performance characteristics of a low concentrated photovoltaic–thermoelectric hybrid power generation device. *International Journal of Thermal Sciences* 77, pp. 158-164.
4. T. Liao et al. Performance characteristics of a low concentrated photovoltaic–thermoelectric hybrid power generation device. *International Journal of Thermal Sciences* 77, pp. 158-164 (2014).
5. X. Xu et al. Performance Analysis of a Combination System of Concentrating Photovoltaic/Thermal Collector and Thermoelectric Generators. *Journal of Electronic Packaging* 136(4), pp. 041004-041004 (2014).
6. D.M. Rowe, and G. Min. Design theory of thermoelectric modules for electrical power generation. *IEE Proceedings - Science, Measurement and Technology* 143(6), pp. 351-356 (1996).
7. F. Attivissimo et al. Feasibility of a Photovoltaic Thermoelectric Generator: Performance Analysis and Simulation Results. *IEEE Transactions on Instrumentation and Measurement* 64(5), pp. 1158-1169 (2015).
8. J. Lin et al. Performance analysis and load matching of a photovoltaic–thermoelectric hybrid system. *Energy Conversion and Management* 105, pp. 891-899 (2015).
9. J. Zhang et al. A novel choice for the photovoltaic–thermoelectric hybrid system: the perovskite solar cell. *International Journal of Energy Research* (2016).
10. R. Lamba and S.C. Kaushik. Modeling and performance analysis of a concentrated photovoltaic–thermoelectric hybrid power generation system. *Energy Conversion and Management* 115, pp. 288-298 (2016).
11. H. Hashim et al. Model for geometry optimisation of thermoelectric devices in a hybrid PV/TE system. *Renewable Energy* 87, Part 1, pp. 458-463 (2016).
12. D. Narducci and B. Lorenzi. Challenges and Perspectives in Tandem Thermoelectric and Photovoltaic Solar Energy Conversion. *IEEE Transactions on Nanotechnology* 15(3), pp. 348-355 (2016).

13. O. Beeri et al. Hybrid photovoltaic-thermoelectric system for concentrated solar energy conversion: Experimental realization and modeling. *Journal of Applied Physics* 118(11), p. 115104 (2015).
14. W. Zhu et al. High-performance photovoltaic-thermoelectric hybrid power generation system with optimized thermal management. *Energy* 100, pp. 91-101 (2016).
15. D.N. Kossyvakis et al. Experimental analysis and performance evaluation of a tandem photovoltaic–thermoelectric hybrid system. *Energy Conversion and Management* 117, pp. 490-500 (2016).
16. J. Garcia-Canadas and G. Min, Low frequency impedance spectroscopy analysis of thermoelectric modules. *Journal of Electronic Materials*, Vol 43, No 6, 2014
17. G. Siefer and A.W. Bett A.W., Progress in Photovoltaics: Research and Applications 2014; 22: 515-524.